Journal of Theoretical and Applied Information Technology
31st May 2024. Vol.102. No. 10

ISSN: 1992-8645 www.jatit.org E-ISSN: 1817-3195

A NOISE-ROBUST DESCRIPTOR: APPLICATIONS TO FACE RECOGNITION

ABDELLATIF DAHMOUNI[1], ABDELKAHER AIT ABDELOUAHAD[1] AND HASSAN SILKAN[1]
[1]LAROSERI Laboratory, Faculty of Sciences, University of Chouaib Doukkali, El Jadida, Morocco
E-mail : dahmouni.a@ucd.ac.ma ; aitabdelouahad.a@ucd.ac.ma ; silkan.h@ucd.ac.ma

ABSTRACT

In the field of computer vision research, identifying the distinctive features of image objects remains a persistent challenge, particularly in face recognition. Although most face recognition techniques excel under ideal conditions, they are limited to the various changes that affect the accuracy of face feature extraction, such as variations of lighting, facial expressions, poses, occlusions, and noise. To best circumvent this problem, we propose a new variant of the Local Binary Pattern (LBP) called the Robust Electric Virtual Binary Pattern (REVBP). The main purpose of the REVBP is to improve the noise performance of the Electric Virtual Binary Pattern (EVBP) descriptor using the localized noise coding method. In order to assess the effectiveness of the proposed approach, two processes are used. The first is a comparative study between REVBP and EVBP in terms of recognition rate and processing time. The second involves combining REVBP with various machine learning algorithms, including variants of the Support Vector Machine (SVM). Extensive experiments have shown that REVBP performs better than the original EVBP. They also showed that using learning classifiers provided significant improvements in terms of recognition accuracy, outperforming several alternative methods.

Keywords: *enhanced Local Binary Pattern Histogram (eLBPH); Robust Electric Virtual Binary Pattern (REVBP); Electric Virtual Binary Pattern (EVBP); Support Vector Machine (SVM).*

1. INTRODUCTION

Recently, computer vision has seen spectacular advances thanks to the artificial intelligence. It has opened up new perspectives in many fields such as security, medicine, motion, video, document, speech and even emotion recognition [1]. In the security industry, biometrics is emerging as a growing discipline that exploits a range of biometric modalities such as fingerprints, iris and face recognition. In fact, face recognition is the most crucial biometric modality that has found revolutionary applications in many areas such as territorial security, surveillance, identity management and access control to various IT systems [2]. Face recognition offers several advantages over other biometric modalities by being natural, non-intrusive and simple. However, this has proven to be one of the most complex challenges in pattern recognition, owing to a wide range of factors such as lighting conditions, facial expressions, pose variations, complex backgrounds, motion blur, and other noise factors that can reduce recognition accuracy [3]. The idea of face recognition methods is mainly based on the adoption of algorithms capable of depicting the face using reduced and discriminant descriptions. Several face recognition methods have been proposed and grouped into three primary approaches: holistic, feature-based and the hybrid. Holistic methods, prevalent in the early 1990s, consider the whole face as an input system to achieve face recognition. These methods can be divided into two sub-classes: the first contains the linear subspace methods like Eigenfaces using principal component analysis (PCA,2DPCA) [4], Fisher-faces using linear discriminant analysis (LDA, 2DLDA) [5], independent component analysis (ICA) [6], spectral methods such as discrete wavelet transform (DWT) and discrete cosine transform (DCT) [7]. The second contains the nonlinear subspace methods like kernel-PCA (KPCA) and kernel-LDA (KLDA) [87], locality preserving projection (LPP) [9] and convolutional neural networks (CNNs) [10-11].

In the early 21st century, the emphasis shifted to feature-based methods, which could eventually be subdivided into techniques based on local appearance and techniques based on points of interest. Local appearance-based techniques treat facial images as collections of small vectors, focusing on the facial landmark's components like the nose, mouth, and eyes. They use feature

extraction descriptors such as local binary pattern (LBP) and its variants [12-13], oriented gradient histogram (HOG) [14] and elastic bunch graph matching (EBGM) [15]. Point-of-interest techniques detect key geometric features of the face using specific algorithms such as scale invariant feature transform (SIFT) and speeded-up robust features (SURF) [16]. Later, several face recognition research turned toward the hybrid methods. These combine local and subspace features to maximize recognition performance. For example, Gabor wavelet linear discriminant analysis (GW-LDA) [17], CNNs combined with stacked auto-encoder (SAE) [18] and advanced Walsh-LBP correlation filters (WLBP) [19]. Recently, advances in facial recognition have been driven by deep learning algorithms, mainly convolutional neural networks (CNNs). Depending on the CNN architecture used, deep learning methods are supervised as original CNNs, unsupervised as auto-encoder (AE) [20] and recurrent neural network (RNN) [21] and hybrid as deep neural network (DNN) [22-23].

In this paper, we focus on face recognition in the context of noisy images. For this, we propose to use our new REVBP descriptor to reduce the effects of noise on recognition accuracy. The remainder of this paper is organized as follows: Section 2 presents an overview of related work. Section 3 provides a detailed description of the proposed approach. Section 4 presents and analyses the experimental results carried out using typical databases. Section 5 provides a conclusion and perspectives.

2. RELATED WORKS

2.1 Feature extraction

In the face recognition system, the feature extraction phase aims to use effective methods to generate a reduced and discriminating face representation. The most widely used feature extraction methods are based on local appearance, mainly variants of the popular LBP descriptor. In fact, in their revolutionary work, Ahonen et al proposed to generate an efficient face representation using the spatially enhanced local binary pattern histogram (eLBPH) [13]. In which the face image is divided into several non-overlapping areas, histograms of these areas are computed and concatenated into a single histogram that represents the face feature. Over time, several variants of the LBP descriptor have been proposed, Ahonen et *al.* proposed the Local Phase Quantization (LPQ) [24], which involves quantifying the Fourier transform phase into local regions. Tan et *al.* [25] generalized and improved (LBP) face recognition by introducing the three-level operator known as Local Ternary Pattern (LTP). Zhang et *al.* [26] further extended LBP with the higher-order Local Derivative Pattern (LDP). In the SIFT framework, CS-LBP [27] was designed to achieve a lower dimensionality representation for image matching than SIFT and LBP. Wang et *al.* [28] proposed the Bayesian-LBP which models the LBP coding process as a probability and optimization problem. Rivera et *al.* introduced the Local Directional Number (LDN) based on edge responses and higher directional numbers. Wankou et al [29] developed the Adaptive Local Ternary Pattern (ALTP) and Adaptive Local Ternary Pattern with Central Symmetry (CS-ALTP), inspired by Weber's law, to meet the specific requirements of face recognition. In a more recent development, Issam et al [30] introduced the LDTP, a method that compactly combines contrast and directional pattern features for texture classification. LDTP simultaneously captures local structures using the concepts of local ternary patterns (LTP) and higher order local derivative patterns (LDP), providing valuable texture information. Khoi et *al.* [31] presented a fast face recognition system using Local Binary Pattern Pyramid (PLBP), and Rotation Invariant Local Binary Pattern (RI-LBP). In his work [32], Alaa Eleyan conducted a comprehensive study on the merging of different local statistical algorithms and the contribution of this fusion to improve face recognition performance. More recently, Shekhar Karanwal [33] compares face recognition efficiency of 14 LBP-based descriptors. Xi et **al.** [34] contributed to a new unsupervised deep learning approach, LBP-Network (LBP-Net), by maintaining a topology close to the convolutional neural network (CNN).

2.2 Classification

Classification is a crucial step of face recognition, where the effectiveness depends on both the discriminative of the face features extracted and the robustness of the classifiers used. Over time, various statistical learning-based classifiers have been proposed for face recognition, including Naïve Bayes (NB), Decision Tree (DT), K-Nearest Neighbors (K-NN), Random Forest (RF), Logistic Regression (LR) and Support Vector Machines (SVM) [35]. In particular, this investigation will focus on SVM. Indeed, SVM is a supervised binary machine learning algorithm that employs a set of support vectors located on optimal hyperplanes. The objective of the SVM training step is to identify

vectors that maximize the gap between these hyperplanes. Therefore, face recognition is considered as a multi-class nonlinear problem, requiring the deployment of kernel SVM classifiers implemented using the Support Vector Machine Library (LiBSVM) [36]. Prominent kernel functions in SVM include the polynomial kernel, Gaussian kernel, Gaussian radial basis kernel, and the sigmoid kernel. In addition, polynomial SVMs have been shown to be effective in face recognition over several years, making them the chosen classifiers in this study. Subsequently, they will be juxtaposed with contemporary techniques such as Deep-learning-based classifiers. network (CNN).

2.3 Deep learning

Deep-learning is a supervised technique that has recently made great progress in pattern recognition and computer vision. Among deep-learning architectures, convolutional neural networks (CNNs) stand out for their significant success in various classification fields. Therefore, CNN is a complex network with multiple hidden layers organized hierarchically as filters/kernels/neurons with learnable weights and includes convolution, pooling and fully connected layers. More recently, several pre-trained CNN models are available such as LeNet, Alex-Net, VGG-Net, Google-Net and Res-Net [37]. Several deep face recognition methods have been proposed. Liu et *al.* [38] introduced a deep multi-patch CNN coupled with deep metric learning to extract highly discriminative reduced-dimension features. Ben Fredk et *al.* [39] improved CNN's performance through aggressive data augmentation that adds a large number of varied images to the dataset. They adapted a fusion strategy between soft-max and central loss to achieve better accuracy. Hou et *al.* [40] opted for convolutional denoising autoencoders for feature learning and utilized SVM for classification. Ding et *al.* [41] introduced a Noise-Resistant Network (NR-network) with a multi-entry structure capturing both low-level and high-level facial features. However, overcoming the pooling operations in this design resulted in the loss of facial features, reducing efficiency in noisy environments. Hussein et *al.* [42] proposed to compare the ResNet-50+SVM, VGG-16+SVM and LBPH+SVM approaches. The results demonstrated the superiority of ResNet-50 in terms of accuracy. In a similar vein, Ma et *al.* [43] introduced Robust-LBP Guiding Pooling (G-RLBP) to enhance CNN model accuracy while effectively mitigating the impact of noise. Kamencay et *al.* [44] compared the performance of CNN, PCA, LBPH and KNN where CNN achieved the highest accuracy.

Although feature extraction methods and classification algorithms are powerful tools for face recognition, they each have their own limitations. The different local descriptors, mainly the LBP variants, are sensitive to local lighting variations and noise, while the efficiency of classification algorithms is closely related to the learning phase conditions. Moreover, despite their great success, CNNs require a significant amount of annotated data, which proves to be a significant constraint in terms of time and resources [45]. In this perspective, our approach aims to improve the feature extraction phase in order to achieve a robust, portable and real-time operational face recognition system.

3. PROPOSED APPROACH

The proposed approach operates in two phases. The first will be dedicated to the comparison of EVBP and EVBP traits extraction varieties in a noisy environment. The second will consist in examining the impact of machine learning classifiers, in particular SVMs.

3.1 LBP-based feature extraction

Generally, face description remains an important stage in the recognition process. It aims to improve recognition efficiency by selecting the most intrinsic and discriminative facial features. Several face description techniques have been proposed, notably the LBP descriptor and its different varieties.

3.1.1 Brief review of LBP

The basic LBP operator originally proposed by Ojala et al. [11] as a texture descriptor, and successfully introduced by Ahonen et al. [13] into face recognition. In order to generate a face description, LBP encodes each current pixel according to its neighborhood as the following equations:

$$\mathrm{LBP}_{P,R}(g_0) = \sum_{j=1}^{P} S(g_j - g_0)2^{j-1} \quad (1)$$

$$\text{Where, } S(x) = \begin{cases} 1 & \text{if } x \geq 0 \\ 0 & \text{if } x < 0 \end{cases} \quad (2)$$

g_0 and g_j denote the current and neighboring pixels. P is the total number of neighboring pixels. R is the radius of the neighborhood and S(.) is the sign function.

LBP has exceptional advantages such as its low computational complexity and its invariance to monotonous lighting changes. Nevertheless, it exhibits limitations, particularly local changes in

illumination, background complexity and noise. In order to address some limitations, various LBP variants have been proposed, including the EVBP descriptor [46].

3.1.2 Brief review of EVBP

The Electric Virtual Binary Pattern (EVBP) descriptor is mainly based on modelling the image as a set of local grids occupied by a set of virtual electric charges. This representation describes the local geometric aspect (concavity and convexity) and the local illumination effect (brightness and contrast) on each object area. In addition, the duality (pixel ←→ electric charge) was used to determine the EVBP value of each pixel while evaluating the interactions between each central electric charge and its neighboring charges. The formulation of the EVBP, in neighborhood of P pixels and radius R, is given by the following equations:

- According to each direction $\vec{u}_j$; $j = 1,2,3,4$:

$$\mathrm{EVBP}_{R,\vec{u}_j}(g_j, g_{j+4}) = \frac{Kg_0}{r_{cj}^2}\left|g_j - g_{j+4}\right| \quad (3)$$

$$\text{Where, } r_{0j} = \left\|\overrightarrow{g_0 g_j}\right\| = \begin{cases} R \text{ if } j = 2,4 \\ \sqrt{2}R \text{ if } j = 1,3 \end{cases} \quad (4)$$

- According to each neighborhood:

$$\mathrm{EVBP}(g_0) = \sum_{j=1}^{4} S\left(\mathrm{EVBP}_{\vec{u}_j}(g_j, g_{j+4})\right)(2^{j-1} + 2^{j+3}) \quad (5)$$

$$\text{Where, } S(x) = \begin{cases} 1 \text{ if } x \geq T \\ 0 \text{ if } x < T \end{cases} \quad (6)$$

T is the threshold computed according to the scanning principle.

- Threshold determining:

$$dQ_t = dQ_n + q_0 \underset{\forall i}{\Rightarrow} dQ_t = q_0 + \sum_i q_i \quad (7)$$

$$\exists(q_T, \varepsilon_i)/q_i = q_T \mp \varepsilon_i \underset{\forall i}{\Rightarrow} q_0 + Pq_T + \sum_i \varepsilon_i = 0 \quad (8)$$

The scanning principle involves considering a charge distribution consisting of a positive charge q_0 and a set of negative charges q_n. All charges are placed at the center of the grid. Each negative charge is then progressively shifted toward the grid's edge in proportion to its value. Throughout this process, the total charge, denoted as dQ_t, is maintained. In the scenario where the grid represents a homogeneous area, the dispersion of negative charges occurs uniformly in all four spatial directions. Conversely, if the grid corresponds to a heterogeneous or peak area, the dispersion of negative charges is random. The EVBP thresholds are derived for an ideal scanning. In our case, the threshold (T) is defined as: $T = \frac{K}{P} g_0^2$, allowing to assess geometric and illumination fluctuations around current pixel. Refer to Figure 1.

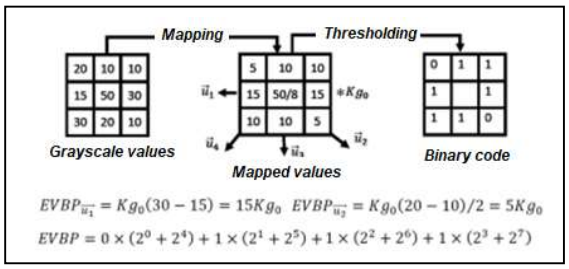

Figure 1: The EVBP calculation

3.2 REVBP-based feature extraction

LBP descriptor and its variants are considered to be the most efficient feature extraction techniques. However, these variants have some limitations, notably sensitivity to different noises. In order to address some of the noise issues, we introduce an improved variant of our EVBP descriptor called Robust-EVBP (REVBP). Which is based on the EVBP principle and the process of classifying noisy pixels in each neighborhood.

3.2.1 REVBP formulation

Generally, LBP varieties such as EVBP descriptor encode each current pixel according to a predefined comparison criterion applied to all its neighboring pixels. When noise affects some neighboring pixels, the resulting code structure is likely to preserve the effect of that noise. In order to minimize the sensitivity of EVBP to noise, we introduced a new descriptor called REVBP. The main idea behind REVBP involves analyzing each current pixel, assessing the likelihood that a neighbor will be affected by noise, and then generating a new code that eliminates the subsequent effect of the noise. Starting from the fact that most LBP-patterns in face images are uniform and that a relatively small proportion are non-uniform [47]. In addition, non-uniform patterns are usually caused by noise. As a result, we can use LBP-patterns to guide the coding process of the current pixel in the direction that reduces the impact of noise. For example, Figure 2 illustrates how to calculate the LBP-patterns of EVBP and REVBP. In this figure the neighbors of pixel (g_c) provided the non-uniform LBP-pattern (01110111). However, the pixel values (g_1=20 and g_5=10) have a high probability of being noisy since they result in sub-pattern of type (101). Replacing 0 by 1 in this sub-pattern results in the uniform LBP-pattern (11111111). Which designates a local spot,

that is a more significant pattern for face representation. The formulation of the REVBP, in neighborhood of P pixels and radius R, is given by the following equations:

- According to each direction $\vec{u}_j$; $j = 1,2,3,4$:

$$\mathrm{REVBP}_{R,\vec{u}_j}(g_j, g_{j+4}) = \mathrm{EVBP}_{R,\vec{u}_j}(g_j, g_{j+4}) \quad (9)$$

$$B_j = B_{j+4} = S\left(\mathrm{REVBP}_{\vec{u}_j}(g_j, g_{j+4})\right); \forall j = 1,2,3,4 \quad (10)$$

$$Sub_k = \begin{cases} B_{k-1}B_kB_{k+1} & \text{if } k = 2,3,4,5,6,7 \\ B_{k-1}B_kB_{k-7} & \text{if } k = 8 \\ B_{k+7}B_kB_{k+1} & \text{if } k = 1 \end{cases} \quad (11)$$

$$\text{Where, } Sub_k = \begin{cases} 000 & \text{if } Sub_k = 010 \\ 111 & \text{if } Sub_k = 101 \\ Sub_k & \text{otherwise} \end{cases} \quad (12)$$

- According to each neighborhood:

$$\mathrm{REVBP}(g_0) = \sum_{j=1}^{4} B_j \times (2^{j-1} + 2^{j+3}) \quad (13)$$

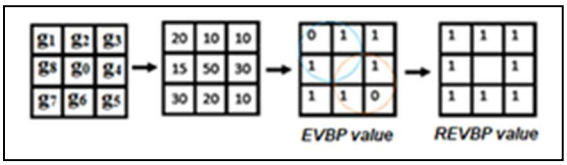

Figure 2: The REVBP calculation

3.2.2 REVBP advantages

In order to highlight the advantages of the REVBP descriptor, we will apply it under the following conditions:

- ✓ Global and local variations in illumination.
- ✓ Noise injection (Gaussian, blur, Poisson, speckle, salt & pepper. . .).
- ✓ Feature length based on the histogram.

As LBP variety, REVBP has low complexity and is invariant to monotonic illumination changes. Moreover, it has other advantages such as invariance with respect to local illumination changes as well as invariance with respect to some noise levels.

- **Lighting invariance:** Regarding the monotonic change of light intensity across the scene (background and foreground), EVBP and REVBP retain original patterns; See (a) transformation in Figure 3. However, in the cases of local changes in light intensity (background or foreground), only EVBP and REVBP produce invariant patterns; See (b) and (c) transformations in Figure 3.
- **Noise invariance:** In comparison to EVBP, REVBP demonstrates robustness in terms of resilience to different noises, including Gaussian, salt and pepper, speckle, Poisson and blur. Indeed, REVBP outperforms EVBP in terms of Gaussian noise, mainly at moderate variance-values (V<0.02). Additionally, REVBP has distinct advantages in handling Poisson noise. When dealing with speckle noise, REVBP produces remarkable results, especially at moderate variance-values (V<0.02). Moreover, when confronted with salt & pepper noise, REVBP performance varies according to the ratio of contaminated pixels, but remains acceptable at moderate variance-values (V<0.05). Finally, REVBP produces remarkable outcomes when confronted with blurred noise, especially at moderate rays (R<5). (Refer to Figure. 4).
- **Feature vector length:** It plays a crucial role in the performance of LBP-based recognition systems, typically addressed using the eLBPH method to build appropriate feature vectors. Initially, the original LBP built feature vectors using 256 bin-histograms. Transitioning to $LBPU^2$ variant reduces this length by 76.95%, to achieve 59 bin-histograms. Likewise, employing EVBP reduces the length by 93.75%, reaching 16 bin-histograms. While, our REVBP further reduces it by 97.66%, achieving only 6 bin-histograms. Further details are given in Table 1.

Table 1: Features Vector Length using eLBPH.

Variety	Nbr-Bins	eLBPH Length	Reduce rate	Ref
LBP	256	7*8*256=14 336	0%	[13]
$LBPU^2$	59	7*8*59=3304	76.95%	[13]
EVBP	16	7*8*16=896	93.75%	[46]
REVBP	6	7*8*6=336	97.66%	Our

3.2.3 Face features extraction

The basic face feature extraction, eLBPH, was first proposed by Ahonen [13]. This involves assembling several descriptions of local face areas to get a global face description. Therefore, each image is divided into [S_1……S_m] non-overlapping sub-images, for which the corresponding histograms are computed and concatenated into a single histogram that represents face feature vector. In our case, we take m=7×8 rectangular areas to obtain a face feature vector of size l=56×6=336. See Figure 5, for more details.

Journal of Theoretical and Applied Information Technology
31st May 2024. Vol.102. No. 10

ISSN: 1992-8645 www.jatit.org E-ISSN: 1817-3195

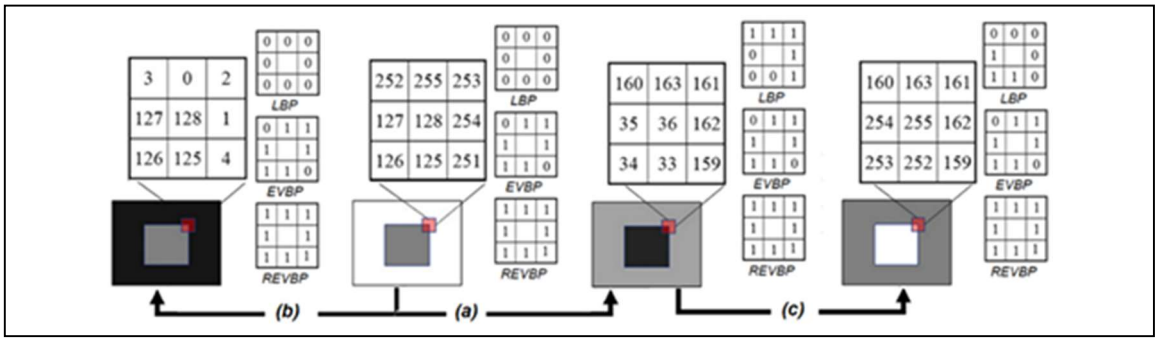

Figure 3: The REVBP lighting invariance.

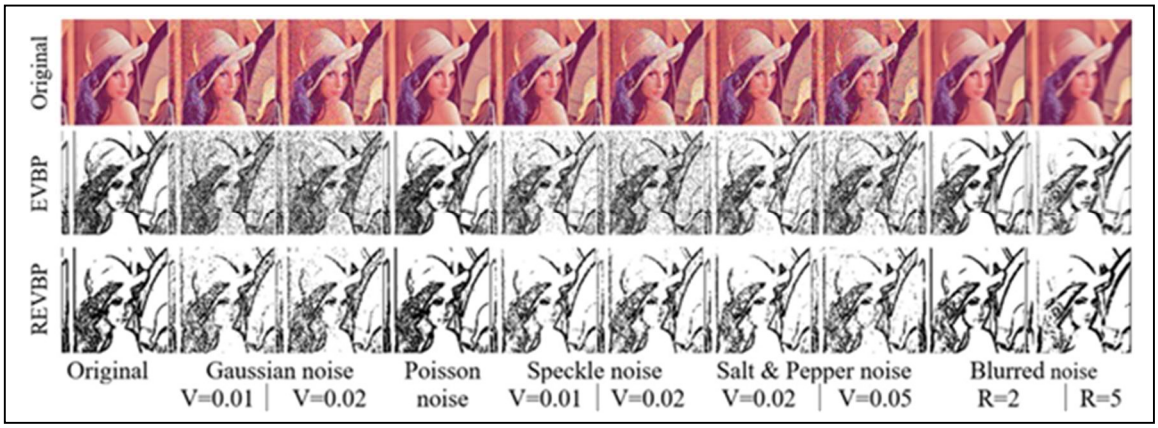

Figure 4: The REVBP noise invariance

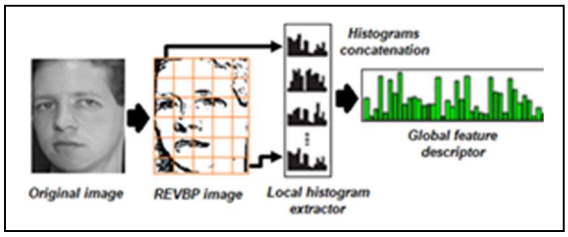

Figure 5: eLBPH face features extraction.

3.2.4 Classification

To classify obtained eLBPH features of each face dataset, two methods are proposed. The first consists to use the Manhattan (L^1) distance defined as:

$$L^1: \quad d_M(H_1, H_2) = \sum_i |H_{1i} - H_{2i}| \qquad (14)$$

The second is to use the following polynomial kernel SVM classifier defined as:

$$K(x_i, x_j) = (x_i . x_j + 1)^d . Where\ d = 1,2,3 \qquad (15)$$

4. EXPERIMENTATION & DISCUSSION

In our experimental investigation, we will assess the suggested approach by conducting a set of experiments using both the ORL and Yale databases with noise and noise-free. The first dataset ORL contains 400 examples from 40 subjects, with 10 grayscale face images of each subject taken under various pose, lighting, and facial expression conditions [48]; See Figure 6. All images have a consistent size of 112×92. The second dataset, named Yale, consists of 165 examples from 15 individuals, each with 11 face images that vary in terms of lighting, facial expressions and other facial details [49]; See Figure 7. All 320×243 images were cropped and resized to 112×92.

Figure 6: Examples of ORL face images.

Journal of Theoretical and Applied Information Technology
31st May 2024. Vol.102. No. 10

ISSN: 1992-8645 www.jatit.org E-ISSN: 1817-3195

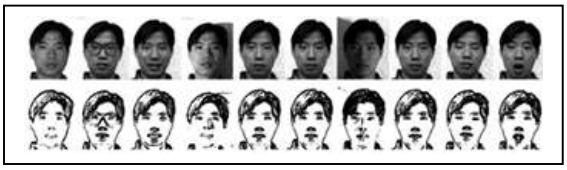

Figure 7: Examples of Yale face images.

4.1 Experiment 1

In the first, we compare the performance of REVBP and EVBP under work-like conditions [46]. Therefore, each image is divided into blocks of 14×14 pixels. Histograms of these blocks are computed and concatenated into a single histogram that represents eLBPH vectors. In addition, the Manhattan metric (L1) is used to measure different eLBPHs similarity. The experimental protocol consists of subdividing each database into a training set and testing set. The training set consists of Ntr images per subject, $N_{tr} \in \{1,3,5,7,9\}$, the remaining images make up the testing set. The comparison between REVBP and EVBP will be made in terms of recognition rate and processing time. The results are shown in Table 2 for the ORL database and Table 3 for the Yale database. Therefore, the results in both Table 2 and Table 3, concerning the without-noise, show that REVBP and EVBP achieved very comparable results in terms of recognition rates. But, REVBP significantly outperforms EVBP in terms of processing time. For example, the following results were reached by REVBP and EVBP using a training set of five images per class. Indeed, using the ORL database, we reach a rate of 95.00% and 96.50% with REVBP and EVBP, respectively. While in terms of processing time, REVBP, with 6.215s, seems to process data much faster than EVBP, with 9.532s. Refer to Table 2. In addition, using the Yale database, we reach a rate of 98.89% and 100.00% with REVBP and EVBP, respectively. While in terms of processing time, REVBP, with 2.410s, appears to process data far more quickly than EVBP, with 3.678s. Refer to Table 3.

Table 2: Comparison results using ORL database.

ORL	EVBP		REVBP	
Ntr	Rate(%)	Time(s)	Rate(%)	Time(s)
1	73.06	9.142	72.22	6.386
3	93.57	9.357	92.14	6.125
5	96.50	9.532	95.00	6.215
7	96.67	9.389	96.67	6.122
9	100.0	8.744	100.0	5.804

Table 3: Comparison results using Yale database.

Yale	EVBP		REVBP	
Ntr	Rate(%)	Time(s)	Rate(%)	Time(s)
1	82.00	3.997	82.67	2.367
3	97.50	3.958	99.17	2.350
5	100.0	3.678	98.89	2.410
7	100.0	3.684	100.0	2.366
9	100.0	3.595	100.0	2.347

In the second, we evaluate the performance of EVBP and REVBP under different noise scenarios. We use a variance of 0.02 for Gaussian and speckle noise, and 0.05 for salt and pepper noise. the radius (R = 5) is applied for blurred noise. In our evaluation procedure, we randomly select, for each database, five images per subject for the training set and use the remaining images for the testing set. The comparison will be made only in terms of the recognition rate obtained using the Manhattan metric (L1) applied to eLBPH vectors. Furthermore, the performance of REVBP and EVBP has been demonstrated against various types of noise. The data in Table 4 indicate that the performances of REVBP and EVBP are comparable for salt and pepper, speckle, Poisson and blur noises. However, for Gaussian noise, REVBP outperforms EVBP particularly for the Yale database. Indeed, for Gaussian noise, REVBP achieved a rate of 95.00% and 94.44% with ORL and Yale databases, respectively. In contrast, EVBP reached a rate of 93.50% and 88.89% respectively for the same databases. In the case of salt and pepper noise, REVBP achieved a rate of 96.00% and 100.00% with ORL and Yale databases respectively. Meanwhile, the EVBP rate respectively reached 94.50% and 98.89%. Regarding speckle noise, REVBP and EVBP achieved respectively 96.50% and 95.50% with ORL database. Hence, both descriptors reached the same rate of 98.89% with the Yale database. For Poisson noise, REVBP achieved a rate of 95.00% and 98.89% with ORL and Yale databases, respectively. While the EVBP reached 96.50% and 100.00% with the same databases. Finally, for blur noise applied to ORL database, REVBP and EVBP achieved a rate of 96.00% and 97.00%, respectively. A rate of 100.00% is reached by both descriptors with the Yale database. Refer to Table 4.

Table 4: Comparison results using ORL and Yale with noise databases.

Databases	ORL		Yale	
Noises	EVBP	REVBP	EVBP	REVBP

Gaussian (V=0.02)	93.50	95.00	88.89	94.44
Salt & pepper (V=0.05)	94.50	96.00	98.89	100.0
Speckle (V=0.02)	95.50	96.50	98.89	98.89
Poisson	96.50	95.00	100.0	98.89
Blur (R=5)	97.00	96.00	100.0	100.0

4.2 Experiment 2

In this experiment, we propose to improve classification phase by using the popular kernel SVM classifier. Thus, we use a polynomial kernel of degree d = 3 and 5-fold cross-validation technique to evaluate performance of REVBP and EVBP with noise and noise-free. Therefore, we compute many performance parameters like accuracy, precision, recall, F-measure, Matthews correlation coefficient (MCC), area under the receiver operating characteristic curve (ROC Area) and area under the precision recall curve (PRC Area) [50]. These parameters are defined as follows:

- ✓ Accuracy: A portion of correct predictions among all model predictions:

$$Accuracy = \frac{\text{TP+}}{\text{TP+TN+FP+FN}} \quad (16)$$

- ✓ Precision: A ratio of true positives to the all-positive predictions. It indicates model's ability to avoid misclassifying negative observations as positive:

$$Precision = \frac{\text{TP}}{\text{TP+}} \quad (17)$$

- ✓ Recall: A ratio of true positives to the all-real positive observations. It measures model's ability to correctly identify all positive observations:

$$Recall = \frac{\text{TP}}{\text{TP+F}} \quad (18)$$

- ✓ F-measure: Harmonic mean of precision and recall:

$$F - measure = \frac{Recall \times Precision}{Recall + Precision} \quad (19)$$

- ✓ MCC: This measure is determined by the correlation coefficient values as:

$$MCC = \frac{TP \times TN - \quad \times FN}{\sqrt{(TP+\quad)(TP+\quad)(TN+FP)(TN+\quad)}} \quad (20)$$

- ✓ ROC Area: A measure of a model's ability to correctly classify classes based on the classification threshold.
- ✓ PRC Area): An alternative measure to the ROC Area, representing precision versus recall at different classification thresholds.

The values of these parameters obtained respectively using the ORL and Yale databases are shown in Tables 5 and 6. In our case, we evaluate and compare different studied models using the F-measure and the Accuracy. According to Table 5's data, which summarizes classification parameters of the ORL database, we conclude that:

- ✓ Without noise, F-Measure and accuracy respectively reached 0,995 and 99.50% for REVBP and 0,984 and 98.50% for EVBP.
- ✓ For salt and pepper noise, they achieved respectively 0,985 and 98.50% for REVBP and 0,964 and 96.50% for EVBP.
- ✓ Their respective values with Blur noise were 0,990 and 99.00% for REVBP and 0,985 and 98.50% for EVBP.
- ✓ With Gaussian noise, F-Measure and accuracy respectively reached 0,985 and 98.50% for REVBP and 0,964 and 96.50% for EVBP.
- ✓ For speckle noise, they achieved respectively 0,990 and 99.00% for REVBP and 0,985 and 98.50% for EVBP.
- ✓ Their respective values with Poisson noise were 0,995 and 99.50% for REVBP and 0,984 and 98.50% for EVBP.

According to Table 6's data, which recapitulates classification parameters of the Yale database, we also conclude that:

- ✓ Noise-free, F-Measure and accuracy respectively reached 0,994 and 99.39% for REVBP and EVBP.
- ✓ For salt and pepper noise, they achieved respectively 0,994 and 99.39% for REVBP and 0,976 and 97.57% for EVBP.
- ✓ Their respective values with Blur noise were 0,982 and 98.18% for REVBP and 0,988 and 98.79% for EVBP.
- ✓ With Gaussian noise, F-Measure and accuracy respectively reached 0,900 and 89.69% for REVBP and 0,833 and 83.03% for EVBP.
- ✓ For speckle noise, they achieved respectively 0,994 and 99.39% for REVBP and 0,976 and 97.57% for EVBP.
- ✓ Their respective values with Poisson noise were 0,970 and 96.96% for REVBP and 0,994 and 99.39% for EVBP.

4.3 Discussions

The previous sections have been dedicated to collecting a set of experimental results, which will now be examined and discussed in order to assess the performance of REVBP against different types of noise. Based on Experiment 1, the results in Tables 2 and 3, without the addition of noise, show a slight difference of 0.015% and 0.011% in recognition rates for the ORL and Yale databases, respectively. On the other hand, it is noteworthy that their processing times differ significantly, with a difference of 0.348% and 0.345% for the ORL and Yale databases, respectively. In short, REVBP seems to process data much faster than EVBP, while maintaining similar recognition performance. In addition, the illustrated results in Table 4, taking into account the addition of noise, show that REVBP is more robust to various type of noise, mainly Gaussian, salt and pepper and speckle where image distortions are very significant.

The results of experiment 2, presented in Table 5, indicate that the polynomial kernel SVM used with the ORL database shows a clear superiority of REVBP compared to EVBP, even in the presence of noise. Similarly, the results in Table 6, concerning the Yale database, show that REVBP and EVBP are very similar, even in the presence of noise. In summary, we have demonstrated that REVBP is an efficient and fast descriptor for processing noisy images, thus showing its effectiveness in face recognition. In addition, the use of the nonlinear SVM classifier with a polynomial kernel allows a better resolution of this recognition problem.

Table 5: Results observed using polynomial-SVM with ORL database.

ORL	Precision	Recall	F-Measure	MCC	ROC Area	PRC Area	Accuracy
EVBP	0,986	0,985	**0,984**	0,985	0,992	0,972	**98.50%**
REVBP	0,995	0,995	**0,995**	0,995	0,997	0,991	**99.50%**
Salt and pepper(V=0.05)							
EVBP	0,968	0,965	**0,964**	0,965	0,982	0,936	**96.50%**
REVBP	0,986	0,985	**0,985**	0,985	0,992	0,972	**98.50%**
Blur(R=5)							
EVBP	0,986	0,985	**0,985**	0,985	0,992	0,972	**98.50%**
REVBP	0,991	0,990	**0,990**	0,990	0,995	0,982	**99.00%**
Gaussian (V=0.02)							
EVBP	0,960	0,955	**0,955**	0,955	0,977	0,918	**95.50%**
REVBP	0,982	0,980	**0,980**	0,980	0,990	0,962	**98.00%**
Speckle(V=0.02)							
EVBP	0,969	0,968	**0,967**	0,967	0,983	0,939	**96.75%**
REVBP	0,986	0,985	**0,985**	0,985	0,992	0,972	**98.50%**
Poisson							
EVBP	0,986	0,985	**0,984**	0,985	0,992	0,972	**98.50%**
REVBP	0,995	0,995	**0,995**	0,995	0,997	0,991	**99.50%**

Table 6: Results observed using polynomial-SVM with Yale database.

Yale	Precision	Recall	F-Measure	MCC	ROC Area	PRC Area	Accuracy
EVBP	0,994	0,994	**0,994**	0,994	0,997	0,989	**99.39%**
REVBP	0,994	0,994	**0,994**	0,994	0,997	0,989	**99.39%**
Salt and pepper(V=0.05)							
EVBP	0,978	0,976	**0,976**	0,975	0,987	0,955	**97.57%**
REVBP	0,994	0,994	**0,994**	0,994	0,997	0,989	**99.39%**
Blur(R=5)							
EVBP	0,988	0,988	**0,988**	0,987	0,994	0,978	**98.79%**
REVBP	0,983	0,982	**0,982**	0,981	0,990	0,966	**98.18%**
Gaussian (V=0.02)							
EVBP	0,848	0,830	**0,833**	0,825	0,909	0,717	**83.03%**
REVBP	0,911	0,897	**0,900**	0,895	0,945	0,827	**89.69%**
Speckle(V=0.02)							

EVBP	0,977	0,976	**0,976**	0,974	0,987	0,955	**97.57%**
REVBP	0,994	0,994	**0,994**	0,994	0,997	0,989	**99.39%**
Poisson							
EVBP	0,994	0,994	**0,994**	0,994	0,997	0,989	**99.39%**
REVBP	0,974	0,970	**0,970**	0,969	0,984	0,946	**96.96%**

4.4 Comparison with the state-of-the-art

The comparison of our approach with state-of-the-art face recognition methods is presented in Table 7. Indeed, for the noise-free ORL database, our approach shows 1,01%, 2,00% and 4,73% higher accuracy than HMM [51], KMCNN [17] and 2DCLDA [55], respectively. With noise added, it outperforms KMCNN [17] and 2DCLDA [55] by 3,55% and 3,.37%, respectively. It is also highly competitive with the DL-MB-LBP method [52]. Concerning the noise-free Yale database, our approach displays a higher accuracy of 5,24%, 5,62%, 1,64% and 1,64% compared to HMM [51], GAN [53], DDTL [54] and 2DCLDA [55], respectively. With noise added, it outperforms 2DCLDA [55] by 2,74%.

Table 7: Comparison results with others methods.

Methods	Databases	Accuracy
HMM [51]	ORL (Noise-free)	98.50%
	Yale (Noise-free)	94.44%
KMCNN [17]	ORL (With noise)	95.12%
	ORL (Noise-free)	97.56%
DL- MB-LBP [52]	ORL (With noise)	98.60%
	ORL (Noise-free)	99.50%
GAN [53]	Yale (Noise-free)	94.1%
DDTL [54]	Yale (Noise-free)	97.78%
2DCLDA [55]	ORL (Noise-free)	95.00%
	Yale (Noise-free)	97.78%
	ORL (With noise)	95.18 %
	Yale (With noise)	96.73 %
Our approach	ORL (Noise-free)	99.50%
	Yale (Noise-free)	99.39%
	ORL (With noise)	98.50%
	Yale (With noise)	99.39%

5. CONCLUSION

In this paper, a new feature extraction method called REVBP was proposed for the noisy environment. The face recognition system had two stages: feature extraction, followed by recognition using an optimized SVM classifier. We have shown that REVBP outperforms its predecessors EVBP in terms of recognition rate and processing time, especially in noisy environments. The proposed method was evaluated using two face databases, ORL and Yale, under two separate scenarios. In the first scenario, the performances of REVBP and EVBP were compared using the Manhattan distance to measure the similarity of feature vectors constructed by the eLBPH method. The results showed that REVBP, in addition to its robustness and speed, is insensitive to noise. In the second scenario, the efficiency of REVBP was improved by using the SVM classifier with a polynomial kernel.

The achieved results were analyzed and compared with those of other advanced methods. They confirmed the robustness of REVBP, with high values for various classification parameters, in particular F-measure and accuracy. For the ORL database, the recorded values are 0,995 and 99.50% respectively, while for the Yale database they achieved 0,994 and 99.39%, respectively. However, this model presents some limitations in uncontrolled environments where the extraction of discriminative face features is complex. These challenges could be solved in the future using a variant of deep learning algorithms. Additionally, we plan to apply proposed approach in IT security, particularly for face spoofing applications.

REFERENCES:

[1] Jain, A. K., Nandakumar, K., Ross, A. (2016). 50 years of biometric research: Accomplishments, challenges, and opportunities. Pattern recognition letters, 79, 80-105.

[2] Lien, C. W., & Vhaduri, S. (2023). Challenges and Opportunities of Biometric User Authentication in The Age of IOT: A Survey. ACM Computing Surveys, 56(1), 1-37.

[3] Adjabi, I., Ouahabi, A., Benzaoui, A., & Taleb-Ahmed, A. (2020). Past, Present, and Future of Face Recognition: A Review. Electronics, 9(8), 1188.

[4] Maafiri, A., & Chougdali, K. (2021). Robust Face Recognition Based on A New Kernel-PCA Using RRQR Factorization. Intelligent Data Analysis, 25(5), 1233-1245.

[5] Alsaqre, F. (2022, May). Fractional Two-Dimensional Linear Discriminant Analysis. In

2022 International Conference for Natural and Applied Sciences (ICNAS) (pp. 70-75). IEEE.

[6] Kumar, A. D., Revathi, N., Sherly, S. I., Lalitha, R., & Raja, R. V. (2023). Innovative Time Series-Based ECG Feature Extraction for Heart Disease Risk Assessment. Journal of Theoretical and Applied Information Technology, 101(21).

[7] Vishwakarma, V. P., & Dalal, S. (2020). Generalized DCT and DWT Hybridization based Robust Feature Extraction for Face Recognition. Journal of Information and Optimization Sciences, 41(1), 61-72.

[8] Poojashree, L. R. (2020). Subspace based Face Recognition: A Literature Survey. Innovative Data Communication Technologies and Application: ICIDCA 2019, 46, 284.

[9] Kumar, N., & Rawat, M. (2020). RP-LPP: A Random Permutation Based Locality Preserving Projection for Cancelable Biometric Recognition. Multimedia Tools and Applications, 79(3), 2363-2381.

[10] Ben Fredj, H., Bouguezzi, S., & Souani, C. (2021). Face Recognition in Unconstrained Environment with CNN. The Visual Computer, 37(2), 217-226.

[11] Thamrin, M., & Darniati, M. A. (2023). Intelligent Security System Based on Biometric Face Recognition. Journal of Theoretical and Applied Information Technology, 101(17).

[12] Ojala T, Pietikäinen M, Maenpaa T (2002) Multiresolution gray-scale and rotation invariant texture classification with local binary patterns. IEEE Trans Pattern Analysis and Machine Intelligence 24(7):971–987.

[13] Ahonen, T., Hadid, A., & Pietikainen, M. (2006). Face Description with Local Binary Patterns: Application to Face Recognition. IEEE Transactions on Pattern Analysis and Machine Intelligence, 28(12), 2037-2041.

[14] Ghorbani, M., Targhi, A. T., & Dehshibi, M. M. (2015, October). HOG and LBP: Towards A Robust Face Recognition System. In 2015 Tenth International Conference on Digital Information Management (ICDIM) (pp. 138-141). IEEE.

[15] Wiskott, L., Fellous, J. M., Krüger, N., & Von Der Malsburg, C. (2022). Face Recognition by Elastic Bunch Graph Matching. In Intelligent Biometric Techniques in Fingerprint and Face Recognition (pp. 355-396).

[16] Gupta, S., Thakur, K., & Kumar, M. (2021). 2d-Human Face Recognition using Sift and Surf Descriptors of Face's Feature Regions. The Visual Computer, 37(3), 447-456.

[17] El Madmoune, Y., El Ouariachi, I., Zenkouar, K., & Zahi, A. (2023). Robust Face Recognition Using Convolutional Neural Networks Combined with Krawtchouk Moments. International Journal of Electrical & Computer Engineering (2088-8708), 13(4).

[18] Wang, H., Hu, J., & Deng, W. (2017). Face Feature Extraction: A Complete Review. IEEE Access, 6, 6001-6039.

[19] Kortli, Y., Jridi, M., Al Falou, A., & Atri, M. (2020). Face Recognition Systems: A Survey. Sensors, 20(2), 342.

[20] Sajid, M., Ali, N., Ratyal, N. I., Usman, M., Butt, F. M., Riaz, I., ... & Ahmad Salaria, U. (2022). Deep Learning in Age-Invariant Face Recognition: A Comparative Study. The Computer Journal, 65(4), 940-972.

[21] Arora, A., & Miri, R. (2020, December). Taylor-Grey Rider Based Deep Recurrent Neural Network using Feature Level Fusion for Cryptography Enabled Biometric System. In 2020 3rd International Conference on Intelligent Sustainable Systems (ICISS) (pp. 807-814). IEEE.

[22] Gondosiswojo, A. R. P., & Kusuma, G. P. (2023). Low Resolution Face Recognition on CCTV Images using a Combination of Super Resolution and Face Recognition Models. Journal of Theoretical and Applied Information Technology, 101(20).

[23] Tong, J. X., Li, H., & Yin, S. L. (2020). Research On Face Recognition Method Based on Deep Neural Network. International Journal of Electronics and Information Engineering, 12(4), 182-188.

[24] Ahonen, T., Rahtu, E., Ojansivu, V., & Heikkila, J. (2008, December). Recognition of Blurred Faces Using Local Phase Quantization. In 2008 19th International Conference on Pattern Recognition (pp. 1-4). IEEE.

[25] Raghavendra, R. J., & Kunte, R. S. (2020). Extended Local Ternary Pattern for Face Anti-Spoofing. Advances in Cybernetics, Cognition, and Machine Learning for Communication Technologies, 221-229.

[26] Kas, M., El-Merabet, Y., Ruichek, Y., & Messoussi, R. (2020). A Comprehensive Comparative Study of Handcrafted Methods for Face Recognition LBP-Like and Non-LBP Operators. Multimedia Tools and Applications, 79(1), 375-413.

[27] Karanwal, S., & Diwakar, M. (2021). OD-LBP: Orthogonal Difference-Local Binary Pattern for

Face Recognition. Digital Signal Processing, 110, 102948.

[28] He, C., Ahonen, T., & Pietikainen, M. (2008, December). A Bayesian Local Binary Pattern Texture Descriptor. In 2008 19th International Conference on Pattern Recognition (pp. 1-4). IEEE.

[29] Yang, W., Wang, Z., & Zhang, B. (2016). Face Recognition Using Adaptive Local Ternary Patterns Method. Neurocomputing, 213, 183-190.

[30] Kas, M., El Merabet, Y., Ruichek, Y., & Messoussi, R. (2019, March). Survey On Local Binary Pattern Descriptors for Face Recognition. In Proceedings of The New Challenges in Data Sciences: Acts of The Second Conference of the Moroccan Classification Society (pp. 1-6).

[31] Khoi, P., Thien, L. H., & Vo, H. V. (2016). Face Retrieval Based on Local Binary Pattern and its Variants: A Comprehensive Study. International Journal of Advanced Computer Science and Applications, 7(6).

[32] Eleyan, A. (2023). Statistical Local Descriptors for Face Recognition: A Comprehensive Study. Multimedia Tools and Applications, 82(21), 32485-32504.

[33] Karanwal, S. (2021). A Comparative Study Of 14 State of Art Descriptors for Face Recognition. Multimedia Tools and Applications, 80(8), 12195-12234.

[34] Xi, M., Chen, L., Polajnar, D., & Tong, W. (2016, September). Local Binary Pattern Network: A Deep Learning Approach for Face Recognition. In 2016 IEEE International Conference on Image Processing (ICIP) (pp. 3224-3228). IEEE.

[35] Abdullah, D. M., & Abdulazeez, A. M. (2021). Machine learning applications based on SVM classification a review. Qubahan Academic Journal, 1(2), 81-90.

[36] Chang, C. C., & Lin, C. J. (2011). LIBSVM: a library for support vector machines. ACM transactions on intelligent systems and technology (TIST), 2(3), 1-27.

[37] Almabdy, S., & Elrefaei, L. (2019). Deep convolutional neural network-based approaches for face recognition. Applied Sciences, 9(20), 4397.

[38] Liu, J., Deng, Y., Bai, T., Wei, Z., & Huang, C. (2015). Targeting ultimate accuracy: Face recognition via deep embedding. arXiv preprint arXiv:1506.07310.

[39] Ben Fredj, H., Bouguezzi, S., & Souani, C. (2021). Face recognition in unconstrained environment with CNN. The Visual Computer, 37(2), 217-226.

[40] Hou, Y., Liu, R., Shu, M., & Chen, C. (2023). An ECG denoising method based on adversarial denoising convolutional neural network. Biomedical Signal Processing and Control, 84, 104964.

[41] Ding, Y., Cheng, Y., Cheng, X., Li, B., You, X., & Yuan, X. (2017). Noise-resistant network: a deep-learning method for face recognition under noise. EURASIP Journal on Image and Video Processing, 2017, 1-14.

[42] Hussain, T., Hussain, D., Hussain, I., AlSalman, H., Hussain, S., Ullah, S. S., & Al-Hadhrami, S. (2022). Internet of things with deep learning-based face recognition approach for authentication in control medical systems. Computational and Mathematical Methods in Medicine, 2022.

[43] Ma, Z., Ding, Y., Li, B., & Yuan, X. (2018). Deep cnns with robust lbp guiding pooling for face recognition. Sensors, 18(11), 3876.

[44] Kamencay, P., Benco, M., Mizdos, T., & Radil, R. (2017). A new method for face recognition using convolutional neural network. Advances in Electrical and Electronic Engineering, 15(4), 663-672.

[45] Russakovsky, O., Li, L. J., Fei-Fei, L., et al. (2023). ImageNet large scale visual recognition challenge. International Journal of Computer Vision, 126(9), 1-42.

[46] Dahmouni, A., El Moutaouakil, K., & Satori, K. (2018). Face description using electric virtual binary pattern (EVBP): application to face recognition. Multimedia Tools and Applications, 77, 27471-27489.

[47] Chen, J., Kellokumpu, V., Zhao, G., & Pietikäinen, M. (2013). RLBP: Robust Local Binary Pattern. In BMVC.

[48] The ORL face database at the AT&T http://www.cl.cam.ac.uk/research/dtg/attarchive /facedatabase. Site last visited April 2023.

[49] The Yale Face Database, http://vision.ucsd.edu/ content/ yale-face-database. Site visited April 2023.

[50] D. M. Powers, "Evaluatuion: from precision, recall and F-measure to ROC, informedness, markedness and correlation," J. Mach. Learn. Technol. 2 (1), 37–63 (2011).

[51] Ali, D., Touqir, I., Siddiqui, A. M., Malik, J., & Imran, M. (2022). Face Recognition System

Based on Four State Hidden Markov Model. IEEE Access, 10, pp. 74436-74448.

[52] Lu, K., Liu, Y., & Wu, J. (2021). Face Recognition Based on Multi-scale and Double-Layer MB-LBP Feature Fusion. In *Big Data Analytics for Cyber-Physical System in Smart City: BDCPS 2020, 28-29 December 2020, Shanghai, China* (pp. 1365-1371). Springer Singapore.

[53] Zhang, Z., & Dong, T. (2021). Image Enhancement of Face Recognition Based on GAN. In Big Data Analytics for Cyber-Physical System in Smart City: BDCPS 2020, 28-29 December 2020, Shanghai, China (pp. 494-500). Springer Singapore.

[54] Liao, M., Fan, X., Li, Y., & Gao, M. (2023). Noise-related face image recognition based on double dictionary transform learning. Information Sciences, vol. 630, pp. 98-118.

[55] Li, C. N., Qi, Y. F., Shao, Y. H., Guo, Y. R., & Ye, Y. F. (2021). Robust two-dimensional capped l2, 1-norm linear discriminant analysis with regularization and its applications on image recognition. Engineering Applications of Artificial Intelligence, vol. 104, pp. 104367.